Optical reflectance anisotropy of the Si/Cu(110) surface alloy

2009 J. Phys.: Condens. Matter 21 405003

(http://iopscience.iop.org/0953-8984/21/40/405003)

J. Phys.: Condens. Matter **21** (2009) 405003 (7pp) doi:10.1088/0953-8984/21/40/405003

Optical reflectance anisotropy of the Si/Cu(110) surface alloy

D S Martin

Department of Physics and Surface Science Research Centre, University of Liverpool, L69 7ZE, UK

E-mail: David.Martin@liverpool.ac.uk

Received 21 April 2009, in final form 12 August 2009
Published 8 September 2009
Online at stacks.iop.org/JPhysCM/21/405003

Abstract

Measurements of the optical reflectance anisotropy (RA) of the Si/Cu(110)-c(2 × 2) surface alloy are reported. Significant changes in the RA response of Cu(110) are observed upon the formation of the surface alloy, and with the growth of one-dimensional (1D) anisotropic Si chains on top of the surface alloy. The transitions between the surface states near the Fermi level (E_F) at the $\bar{Y}$ symmetry point on the clean Cu(110) surface are no longer observed in RA spectra of 0.3 ML Si coverage. Peaks in RA spectra arising from transitions between surface-modified bands near E_F at the L point are found to be sensitive to the formation of the surface alloy. The RA response of the c(2 × 2) surface alloy from 3.0 to 5.5 eV is simulated using a simple three-phase derivative model. The addition of an overlayer phase to this model makes it possible to simulate higher coverage Si/Cu RA profiles where 1D Si chains cover the surface alloy. The success of the models, in which discrete phases contribute to the RA response, supports the view that the Si chains grow on top of the intact c(2 × 2) alloy. Depositing between 1.2 and 1.8 ML Si results in no change to the RA spectroscopy signal, indicating that the signal remains sensitive to the covered alloy interface.

(Some figures in this article are in colour only in the electronic version)

1. Introduction

Two-dimensional (2D) surface alloys, created by incorporating atoms of one element into the surface of a crystal substrate composed of a different element, offer a route to the tailoring of surfaces for a variety of fundamental and technological applications [1–3]. The deposition of Si onto the Cu(110) surface has attracted interest [4–13] as one of the first ordered surface alloys to be observed for the deposition of a semiconductor onto a metal surface. The majority of the previous studies [4–12] have focused on investigating surface atomic structure, establishing that following the deposition of 0.5 monolayer (ML) of Si onto Cu(110) at room temperature an ordered surface alloy with c(2 × 2) structure is completed. The structure, first proposed by Martín-Gago *et al* [4], is shown in figure 1. The Si atoms substitute alternate Cu atoms from the close-packed [1$\bar{1}$0] rows in the outermost layer [4–8]. Further deposition of Si results in the formation of linear atomic chains of Si on top of the c(2 × 2) structure and aligned along the [1$\bar{1}$0] surface direction [10] as shown in figure 1. These one-dimensional (1D) chains have been observed between 0.55 and 0.8 ML Si coverage with the number of chains per unit area increasing with increasing coverage [10]. Neighbouring chains are separated by integer distances along [001], the most common being twice that of the Cu surface unit cell in [001]. Adjacent Si atoms within a chain are separated by twice the Cu unit cell length along [1$\bar{1}$0].

In the work presented here, the optical properties of the Si/Cu(110) surface are investigated using reflection anisotropy spectroscopy (RAS) [14–16]. RAS is a linear optical spectroscopy that probes Δr, the difference in normal incidence reflectance for orthogonal linear polarizations, normalized to the mean reflectance r. The real part of the complex reflectance anisotropy (RA) response is measured, defined as

$$\mathrm{Re}\left(\frac{\Delta r}{r}\right) = \mathrm{Re}\left(\frac{2\{r_x - r_y\}}{r_x + r_y}\right) \approx \frac{R_x - R_y}{R_x + R_y} \qquad (1)$$

where r_x represents the complex Fresnel reflection amplitude, and R_x the reflectivity, for x polarization. The system is aligned such that x and y align along the Cu(110) surface

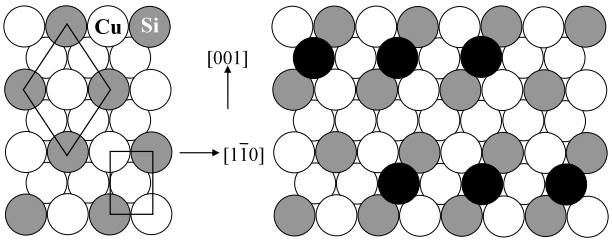

Figure 1. Top-view schematic showing surface atomic structure. Left: the Si/Cu(110) c(2 × 2) surface alloy. The surface unit cell for Cu(110) (rectangle) and the alloy (diamond) are shown. Right: linear Si chains (black) on top of the c(2 × 2) structure.

directions [1$\bar{1}$0] and [001] respectively (figure 1). The RAS technique was originally developed as a real-time probe of semiconductor growth [14] and over the last two decades RAS has emerged as a powerful probe of metallic systems [16]. When RAS is applied to a cubic crystal of isotropic bulk optical response, the RA arises in the surface region making RAS a surface sensitive optical technique. RAS has been used to investigate the bi-metallic surface alloys Pd/Cu(110) [17, 18] and Pd/Au(110) [19]. In the work presented here significant changes in the RA response of the Cu(110) surface are observed upon alloying with Si, and with the growth of anisotropic 1D Si chains on top of the surface alloy. The surface alloy phase and the Si chains produce distinct and characteristic features in the RA spectra. It is found that the RA response can be simulated using simple three- and four-phase models and the results indicate that at higher coverage the c(2 × 2) surface alloy exists intact underneath the Si chains.

2. Experimental details

The experiments were performed in an ultrahigh vacuum (UHV) environment with a base pressure in the 10^{-10} mbar region. Two different Cu(110) high quality single crystal specimens (SPL Netherlands) were used that were aligned to ∼0.1° and mechanically polished to a mirror smooth finish before introduction into UHV. Clean Cu(110) surfaces were prepared in UHV by repeated cycles of Ar ion bombardment (15 min, ∼8 μA, 0.5 kV, 300 K) and annealing to 800 K. Surface atomic order was confirmed by a sharp (1 × 1) low-energy electron diffraction (LEED) pattern and cleanliness was monitored using x-ray photoelectron spectroscopy (XPS) and by the presence of an intense RAS peak at photon energy ∼ 2.1 eV involving transitions between surface states that are sensitive to surface contamination [16]. RA spectra obtained from the two Cu crystals following the deposition of Si were found to display the same characteristic profiles with the same coverage dependence.

An RA spectrometer based upon the Aspnes design [14] utilizing a Xe photon source and photoelastic modulator was coupled to the UHV chamber through a low-strain window. Experimental artefacts were removed from spectra using a correction function obtained by measuring spectra with the specimen in two orthogonal positions. RAS measures anisotropy in reflectance over an area on the Cu crystal of ∼0.5 cm^2. Spectra of the real part of the complex RA were taken over a photon energy range of 1.5–5.5 eV. The deposition source was an Omicron EFM3 evaporator with integral flux monitor loaded with a crystalline Si rod (Goodfellow) of purity 99.999%. Deposition took place with the Cu crystal at room temperature and under conditions of constant deposition flux. Consistent with previous work, the definition of 1 ML as the number of surface Cu atoms in the [1$\bar{1}$0] rows is adopted so that a Si coverage $\theta = 0.5$ ML is the completed c(2 × 2) alloy (figure 1). Previous studies [5, 7, 8] have established that characteristic LEED patterns are observed as the coverage increases to 0.8 ML. Following deposition of 0.25 ML of Si onto Cu(110) a c(2 × 2) pattern is observed with broad half-order spots that are elongated along the [001] surface direction. The half-order spots narrow with further coverage and reach a maximum intensity and sharpness at 0.5 ML [4, 7, 8, 10]. Coverage is determined by comparing LEED data with the previous LEED studies [8, 10] and by an analysis of the ratios of the Cu 3s, 3p and Si 2p XPS peaks using a simple overlayer model. The error on the coverage is estimated to be 0.05 ML. Scanning tunnelling microscopy (STM) was performed in constant current mode using an Omicron STM. A tunnelling current of 1 nA and bias voltages in the range −0.5 to −1.0 V were used. STM tips were made from electrochemically etched tungsten wire.

3. Results and discussion

3.1. Overview of the clean Cu(110) surface

The RA spectrum of the clean Cu(110) surface, shown by curve (a) in figure 2, has been the subject of a number of studies (for a review, see [16]). The main features of the spectrum have been associated with specific optical transitions summarized as follows. The intense RAS peak at ∼2.1 eV arises primarily from transitions between two surface states [20, 21] located near the Fermi level (E_F) at the $\bar{Y}$ point of the surface Brillouin zone. Transitions between bands near E_F at the L symmetry point, that are modified by the anisotropic surface, contribute to the RA response: the peaks observed at 4.25 eV and 4.9 eV have been assigned [22] to the optical transitions $E_F \rightarrow L_1^u$ and $L_2' \rightarrow L_1^u$, respectively. Equivalent transitions have been associated with peaks observed in the RA spectrum of the (110) surfaces of Au [23] and Ag [24]. The temperature dependence of the energy position of these RAS peaks, for Cu, Au and Ag, was found to agree with the temperature dependence of the transition energies between the associated bands, as determined from thermovariation optical spectroscopy [25]. First principles calculations of the RA response of Cu(110) have also indicated that the RAS response between 3.0 and 5.5 eV is associated with transitions involving bulk bands [26–30], and that contributions may not be limited to high symmetry points but may also come from parallel bands elsewhere in the Brillouin zone [29].

3.2. Surface alloying, $0 < \theta \leqslant 0.50$ ML

Significant changes in the RA response are observed upon Si deposition, as shown in figure 2. The first changes to

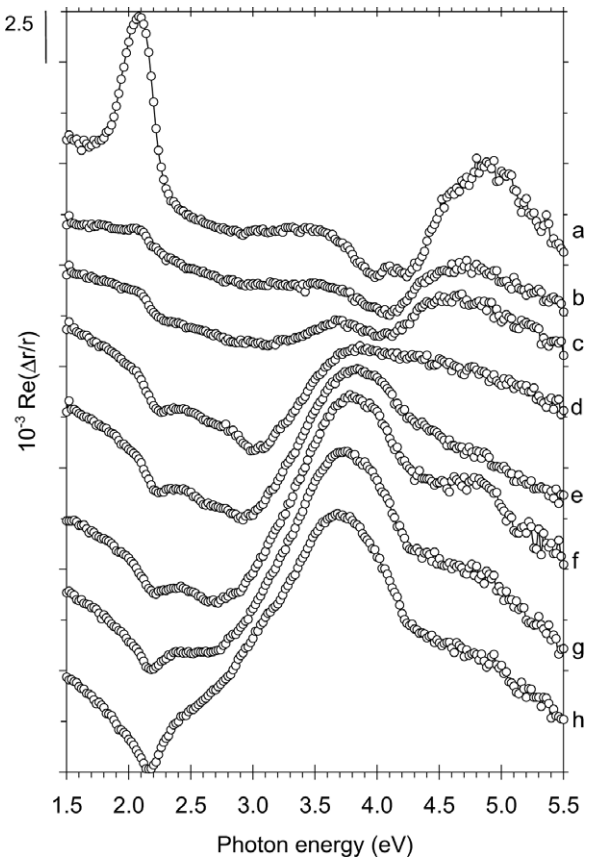

Figure 2. RA spectra following the deposition of Si onto Cu(110). (a) clean Cu(110). ((b)–(h)) Increasing Si deposition: (b) 0.3 ML, (c) 0.4 ML, (d) 0.55 ML, (e) 0.7 ML, (f) 0.85 ML, (g) 1.0 ML, (h) 1.2 ML $\leqslant \theta \leqslant$ 1.8 ML. Successive spectra are offset on the vertical scale for clarity.

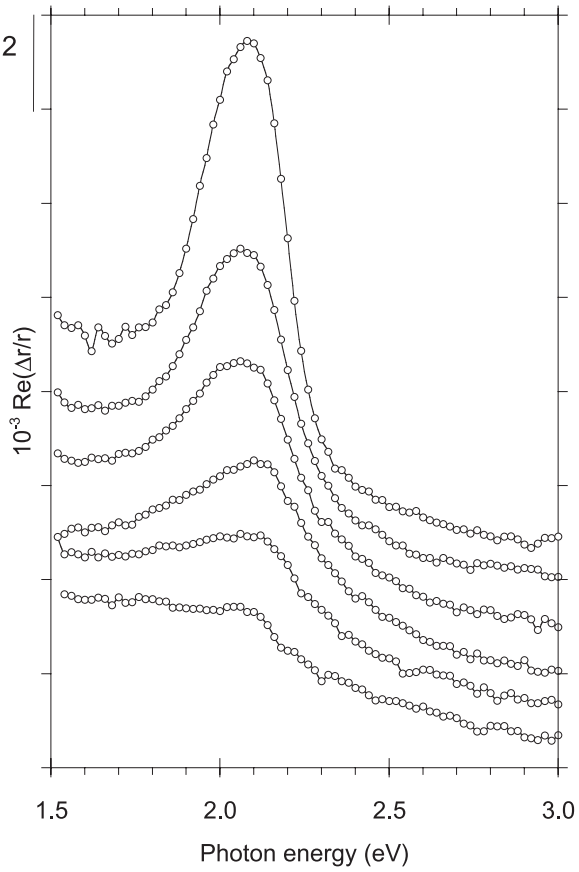

Figure 3. RA spectra showing the decay of the 2.1 eV peak with increasing Si deposition. Successive spectra are offset down the vertical scale for clarity following the sequence $\theta = 0$, 0.05, 0.10, 0.15, 0.20 and 0.30 ML.

be observed following the deposition of up to 0.3 ML Si (figure 2(a) and (b)) are (i) the 2.1 eV peak is quenched, (ii) the peaks at 4 and 4.25 eV of the clean surface are replaced by a single peak at 4.1 eV, and (iii) the 4.9 eV peak of the clean surface shifts to 4.7 eV. The peaks found at 4.1 and 4.7 eV for $\theta = 0.3$ ML have shifted to these energies already for the $\theta = 0.1$ ML surface and shift only a further 0.05 eV upon increasing θ to 0.4 ML (figure 2(c)). The shifts to lower energy of the these peaks associated with the interband transitions at L show that these transitions are sensitive to the formation of the surface alloy. Sensitivity of these transitions to the surface structure including lattice expansion [25, 31] and the creation of vacancies via ion bombardment [32, 33] has previously been demonstrated. For Si/Cu(110), alloying occurs locally from ∼0.04 ML Si coverage [7–9] and strong bonding is thought to be responsible for an initial relaxation of the alloy structure along [001] [8] and the completed alloy layer adopting a buckled corrugation where the Si atoms are located slightly deeper in the surface layer than the Cu atoms [5, 6, 11]. The buckled morphology appears responsible for the RAS peak shifts in the spectral region 4–5 eV. This will be considered further in section 3.4.

The quenching in intensity of the 2.1 eV RAS peak is shown in detail in figure 3. Following the loss of most of the initial intensity, a shoulder feature centred at 2.15 eV is observed for $\theta = 0.3$ ML. It is concluded that the transitions involving the two surface states at $\bar{Y}$ have been lost for $\theta = 0.3$ ML. It is noted that the surface state located at 0.4 eV below E_F at the $\bar{\Gamma}$ point of Cu(111) is no longer observed in photoemission spectra following deposition of a few angstrom thickness of Si [34]. With further Si deposition the shoulder at 2.15 eV begins its development into the negative peak seen at higher coverage (figure 2).

3.3. Anisotropic Si chains, $\theta > 0.5$ ML

The RA spectrum of the $\theta = 0.55$ ML surface is shown in figure 2(d). At this coverage, a positive RAS peak is observed at 3.9 eV which will develop more clearly as a peak with further coverage (figure 2), and a negative RAS peak is observed at 3 eV. A normal emission valence band photoemission study [13] has found evidence that the c(2 × 2) alloy phase has associated with it two surface states at binding energies −1.2 and −0.9 eV. The photoemission peaks of these states have a maximum intensity for 0.5 ML Si and are not clearly observed in 0.3 and 0.9 ML data [13]. The same study predicts theoretically the existence of an unoccupied state at 1.6 eV above E_F. It is now considered whether transitions between these states could contribute to the RAS profile. Such

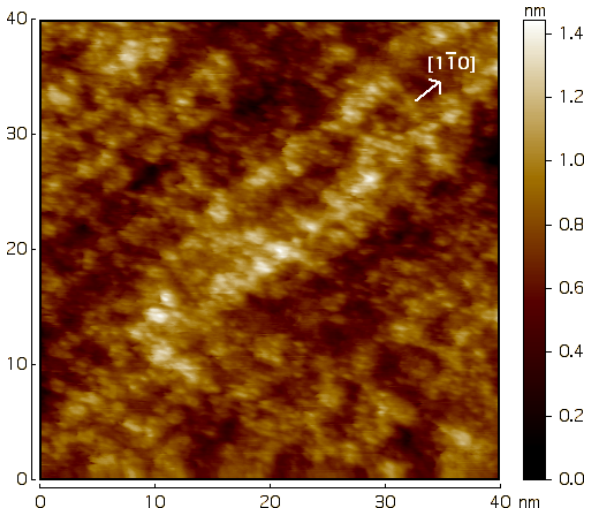

Figure 4. STM image of the high coverage $\theta = 1.5$ ML surface.

a RAS peak would be expected near ∼2.6 eV. Both occupied states are thought to derive from a combination of p_x and p_y bonding orbitals and the unoccupied state of mainly s type [13]. As the two occupied states are close in energy, and have orthogonal symmetries, it is possible that their contributions may cancel each other out in the RAS measurement [16]. A small negative RAS peak at ∼3 eV does develop into a distinct maximum at $\theta = 0.55$ ML and with further deposition it is no longer observed as a distinct peak (figure 2). It is possible, but by no means conclusive, that this peak is related to surface state transitions.

RAS results for $\theta > 0.55$ ML Si are shown by the profiles (e)–(h) in figure 2. With increasing coverage the negative peak at 2.2 eV increases in intensity and becomes more symmetrical in shape. The negative peak at 3 eV observed at 0.55 ML (figure 2(d)) is no longer observed as a distinct peak with further deposition. A large and broad positive peak develops that dominates the spectrum at higher coverages (figure 2(e)–(h)). This peak increases in intensity and shifts to lower energy with increasing coverage, residing at 3.7 eV in profile 2(h).

LEED results of the $\theta = 0.85$ ML surface that gives rise to the RAS profile of figure 2(f) show a c(2 × 2) pattern with faint and continuous streaks in the real space [001] direction that cross the diffraction spots. The pattern is very similar to that reported by Polop *et al* [10] for 0.8 ML coverage. Streaking along [001] is observed for coverage above 0.5 ML and indicates the presence of the linear Si atomic chains on top of the c(2 × 2) structure, as shown in figure 1 [4, 10]. STM results by Polop *et al* [10] show that for $\theta = 0.55$ ML the alloyed terraces support a low number density of 1D Si chains aligned along the [1$\bar{1}$0] direction and extending typically 8 nm. For 0.8 ML, a much higher density of Si chains are observed with chains extending typically 10 nm [10]. Different domains of chains can lead to a relative shift by one atomic site in [1$\bar{1}$0]. The variation in the periodicity in the [001] direction is consistent with the streaking observed along [001] in the corresponding LEED pattern. For both coverages, the STM data reveal clusters on top of the terraces and these clusters, along with other defects, appear to initiate chain growth. The sequence of RA spectra from (e) to (h) in figure 2—corresponding to an increase of θ from 0.7 to 1.2 ML—show a gradual development of the RAS features that are present in profile (e), increasing the intensities of the RAS peaks at 2.2 and 3.9 eV. This increase in RAS signal is likely related to the increase in the number of 1D Si chains on top of the c(2 × 2) alloy, which causes an increase in macroscopic anisotropy.

For coverage $\theta = 1.2$ ML, LEED results show that the continuous streaks along [001] observed at 0.85 ML remain, however, the half-order spots are no longer observed. For coverage 1.2 ML $\leqslant \theta \leqslant$ 1.8 ML the RA profiles were indistinguishable and the profile characteristic of this coverage range is shown in figure 2(h). LEED results for coverages 1.5–1.8 ML showed a (1 × 1) pattern at lower beam energy, with a diffuse unstructured background. While the morphology of the surface has been well characterized by STM for $\theta <$ 1 ML [10], no prior data has been reported for higher coverage. Thus, STM was performed on the $\theta = 1.5$ ML surface to gain insight into the morphology of this coverage. The results revealed the occurrence of clustering on top of a surface which retains an overall anisotropy along the [1$\bar{1}$0] direction (figure 4). Clustering, whilst observed for $\theta = 0.55$ ML, becomes dominant at higher coverage. Height ranges of 1.2–1.5 nm were observed over 40 nm × 40 nm areas, although some caution is necessary in interpreting STM height values from a complex alloyed surface. These observations suggest that the deposited Si covers the ordered alloy interface and the 1D Si chains, whilst maintaining significant anisotropy along [1$\bar{1}$0]. The covering may not be complete across the entire surface since the clustering and large height range observed in figure 4 for ∼1 ML deposited onto the surface alloy suggests that the Si is not growing layer-by-layer and there will be regions on the surface where Si chains are not covered by the additional Si.

3.4. Simulating the RAS data

RA spectra of surfaces often derive from a combination of morphological and electronic effects and can therefore be difficult to interpret. Progress can be made by using model systems and several examples of this approach have been reviewed [16]. A common method of simulating RAS data, developed from Fresnel theory by McIntyre and Aspnes [35] is to simplify the system under investigation to that of a three-phase system. The three phases—vacuum, surface and bulk—have their own complex dielectric function, ϵ. The reflection coefficients and $\Delta r/r$ for normal incidence reflection are then determined for the system. For adsorbate systems the three-phase model can be extended to four phases with the addition of an optically anisotropic overlayer, as shown in figure 5. This four-phase model consists of (i) a semi-infinite and isotropic ambient or vacuum ($\epsilon_v = 1$), (ii) a biaxial overlayer ($\Delta\epsilon_o = \epsilon_o^x - \epsilon_o^y$, where $\epsilon_o^x \neq \epsilon_o^y$ and x and y are orthogonal in-plane directions which are aligned along x and y polarizations), (iii) a biaxial surface layer ($\Delta\epsilon_s$) and (iv) a semi-infinite isotropic bulk substrate (ϵ_b). The thickness of the overlayer (d_1) and surface (d_2) are much less than the wavelength of light (λ). To simulate the RAS of clean Cu(110), a three-phase model (no

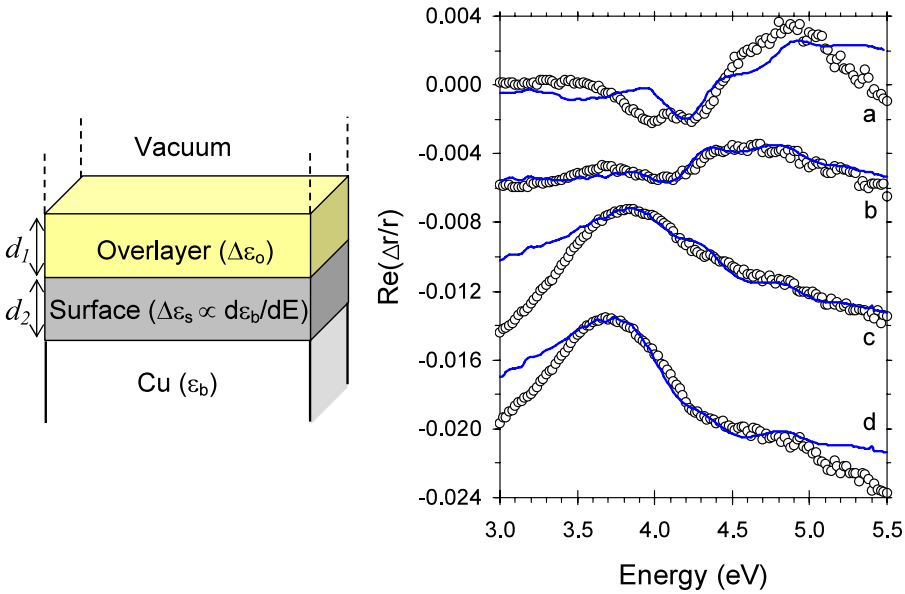

Figure 5. Left panel: four-phase model used to simulate the RAS data. Right panel: experimental (circles) and simulated (solid line) RA spectra: (a) clean Cu(110), (b) $\theta = 0.4$ ML, (c) $\theta = 0.7$ ML and (d) 1.2 ML $\leqslant \theta \leqslant$ 1.8 ML. Profiles (b)–(d) are offset on the vertical scale for clarity.

overlayer phase in figure 5) is often used where $\Delta\epsilon_s$ of the Cu surface is based on the energy derivative of the bulk dielectric function $\mathrm{d}\epsilon_b/\mathrm{d}E$ [36, 37]. The Cu(110) surface is assumed to perturb the electronic structure of the subsurface region, modifying the energies E_g and linewidths Γ of interband transitions at critical points. The structural anisotropy of the Cu(110) surface causes different band narrowing along $[1\bar{1}0]$ and [001] leading to differences in gap energies ΔE_g and linewidths $\Delta\Gamma$ between $[1\bar{1}0]$ and [001] polarizations. For this 'three-phase derivative model' the RAS is given by:

$$\frac{\Delta r}{r} = -\frac{4\pi \mathrm{i} d_2}{\lambda} \frac{(\Delta E_g + \mathrm{i}\Delta\Gamma)}{\epsilon_b - 1} \frac{\mathrm{d}\epsilon_b}{\mathrm{d}E}. \qquad (2)$$

This approach simulates the RA response in the region 3.0–5.5 eV arising from the transitions originating in the vicinity of the L point. Indeed, the (110) surfaces of Cu [22, 33], Au [23, 38, 39] and Ag [24], for both well-ordered and ion bombarded surfaces, have been modelled in terms of the three-phase derivative model of equation (2). Three- and four-phase derivative models are now used to simulate the RAS results of Si/Cu(110) between 3.0 and 5.5 eV. Dielectric properties of single crystal Cu at 0.02 eV energy resolution are used [40].

Firstly, the clean Cu(110) surface is simulated using the three-phase derivative model (no overlayer phase) with $d_2 = 1$ nm, $\Delta E_g = 0.1$ and $\Delta\Gamma = 0$. The result is shown by profile (a) in figure 5. The simulation shows the expected good agreement with experiment with peaks at 4.2 and 4.9 eV occurring close to the experimentally observed peaks. It is found that the Si/Cu(110) RAS results for $\theta < 0.55$ ML can be simulated using the same three-phase derivative model. By varying only the parameters ΔE_g and $\Delta\Gamma$ it is found that the shift to lower energy of the RAS peaks following Si deposition (figure 2(a)–(c)) can be reproduced. Values of $\Delta E_g = 0.02$ eV and $\Delta\Gamma = 0.06$ eV simulate the 0.4 ML Si spectrum as shown in figure 5(b). It is concluded that the effect of surface alloying on the RA response above 3 eV is the modification of the transitions at L. The c(2 × 2) surface alloy adopts a buckled corrugation where the Si atoms are located slightly deeper in the surface layer than the Cu atoms [5, 6, 11]. As the atomic and electronic structure of the Cu surface changes to a buckled Si/Cu surface alloy, the perturbation by the surface on the bands at L also changes, resulting in a change in ΔE_g and $\Delta\Gamma$.

To simulate the RAS results for $\theta > 0.5$ ML, it becomes necessary to use a four-phase model. The overlayer phase in the four-phase model (figure 5) is used to simulate the contribution from the linear Si atomic chains which exist on top of the surface alloy for $\theta > 0.5$ ML (figure 1). The overlayer has a single oscillator of energy ω_t, strength S and width γ occurring for one of the RAS polarizations. It is found that an oscillator for y polarization gives simulated RAS profiles with the same sign as the experiment. For this case, the oscillator is described by [41]

$$\epsilon_o^y = 1 + \frac{S/\pi}{\omega_t - \omega + \mathrm{i}\gamma/2}; \qquad \epsilon_o^x = 1. \qquad (3)$$

The thickness of the overlayer d_1 is set to 1 nm, leaving ω_t, S and γ of the oscillator as free parameters. The thickness d_2, ΔE_g and $\Delta\Gamma$ of the surface phase in the four-phase model (figure 5) are fixed at their values of the fit to $\theta = 0.4$ ML (figure 5(b)). Thus this surface phase with values $d_2 = 1$ nm, $\Delta E_g = 0.02$ eV and $\Delta\Gamma = 0.06$ eV simulates the contribution from the Si/Cu-c(2 × 2) surface alloy. Representing the surface alloy with the 0.4 ML data ensures that no 1D Si chains are present, which form upon any slight excess of Si above 0.5 ML. The surface alloy contribution then remains unchanged with further Si deposition, which includes the assumption that no significant change occurs in ΔE_g and $\Delta\Gamma$ upon increasing

θ from 0.4 to 0.5 ML. The retention of a stable surface alloy phase with further Si deposition is in agreement with experiment [10]. The normal incidence reflectance for x and y polarization, R_x and R_y, from the four-phase structure is calculated from a consideration of the reflection from each interface [42]. The real part of the RAS is then obtained from equation (1). The results of the simulations are shown in figure 5(c) and (d).

The RAS profile of $\theta = 0.7$ ML is simulated using oscillator values $\omega_t = 4.15$ eV, $S = 1.7$ and $\gamma = 1.3$ eV. The simulated profile is shown in figure 5(c). To simulate the RA spectrum of the highest coverage studied, 1.2 ML $\leqslant \theta \leqslant$ 1.8 ML, oscillator values of $\omega_t = 3.95$ eV, $S = 2.2$ and $\gamma = 1.2$ eV are used. The resulting profile is shown in figure 5(d). The simulated spectra reproduce reasonably well the main feature of the experimental spectra—the broad positive peak at 3.9 eV for $\theta = 0.7$ ML, and its shift to lower energy with increasing coverage is reproduced by reducing ω_t. The contribution of the derivative Si/Cu surface layer to the four-phase model is important for the simulation to follow the experimental profile above 4.2 eV, as can be appreciated from the profile of figure 5(b). The simulations of the Si/Cu surfaces diverge from the experimental profiles at lower (<3.5 eV) energy.

The RA spectrum of the $\theta = 0.55$ ML surface (figure 2(d)) shows the first indications of the positive RAS peak at 3.9 eV which develops more clearly as a peak with further coverage. The overall slope from 3.5 to 5.5 eV (figure 2(d)) can be broadly simulated with $\omega_t = 4.15$ eV, $S = 0.9$, $\gamma = 1.3$ eV and ΔE_g, $\Delta\Gamma$ as $\theta = 0.4$ ML. The need to introduce the overlayer to simulate 0.55 ML is consistent with the coverage being slightly above 0.5 ML where some 1D Si chains are present on top of the surface alloy.

For simulating the range 0.55 ML $\leqslant \theta \leqslant$ 1.2 ML, the oscillator strength S increases, γ remains similar and ω_t shifts uniformly to lower energy. In this coverage range, the anisotropic 1D Si chains are forming on top of the completed c(2 × 2) alloy and increase in number density. The increase in RAS signal at ∼3.9 eV, simulated by an increase in S, is likely related to the increase in number density of Si chains with increasing coverage, which causes an increase in macroscopic anisotropy. At $\theta = 0.8$ ML a large number of Si chains cover the surface and it is implied that the increase in the number of chain structures between 0.55 and 0.8 ML will be larger than the increase between 0.8 and 1.2 ML [10]. This view is supported by the RAS simulations where S approximately doubles from 0.55 to 0.85 ML then increases by approximately a third for simulating the 1.2 ML spectrum. Deposition of up to 0.6 ML Si onto the $\theta = 1.2$ ML surface does not change the RA spectrum (figure 2(h)). The deposited Si forms clusters on top of the pre-existing structures (figure 4). The single value of S required to simulate the RAS profile of 1.2 ML $\leqslant \theta \leqslant$ 1.8 ML is consistent with the view that the linear Si chain structures remain intact under the additional Si.

A uniform red-shift is observed in the 3.9 eV RAS peak from 0.55 to 1.2 ML coverage, and this is simulated by reducing ω_t of the oscillator. Over the range 0.55 ML $\leqslant \theta \leqslant$ 1.2 ML some Si is deposited as clusters, on top of the alloy surface and on top of the linear Si chains [10]. Thus there will be Si chains that are free from clusters and Si chains that have clusters deposited on them. The uniform red-shift of the peak associated with Si chains suggests that both free and cluster-covered Si chain structures respond in the same way to the presence of the additional Si. It is interesting to note that Fleischer *et al* [43] have reported a red-shift in the negative RAS peak characteristic of Ag nanostructures grown on Si(111) substrates, following the capping of the nanostructures via deposition of Si. Multilayer simulations indicated the survival of the Ag structures following capping. There are then some similarities in depositing Si onto Ag/Si(111) with depositing Si onto the Si/Cu(110) system.

In summary, between 3.5 and 5.5 eV, a simple three-phase derivative model is found to simulate the surface alloy of the Si/Cu(110) system. A four-phase overlayer derivative model (figure 5) is found to simulate the higher coverage results where 1D Si chains cover the surface alloy. The success of the models, in which discrete phases contribute to the RA response (figure 5), supports the view of Polop *et al* [10] that the Si chains grow on top of the intact c(2 × 2) alloy. Furthermore, both the alloy phase and the Si oscillator phase are found to persist with further Si deposition. The simple optical modelling performed here thus provides some insight into the system. Further information, particularly on the RA response below 3 eV, could come from complimentary first principles calculations of the electronic and optical properties of the Si/Cu(110) system.

4. Conclusions

The optical reflectance anisotropy of the Si/Cu(110)-c(2 × 2) surface alloy, and the anisotropic 1D Si chains on top of the surface alloy, have been investigated. The transitions between the surface states near E_F at $\bar{Y}$ on the clean Cu(110) surface are no longer observed in RA spectra of $\theta = 0.3$ ML. The RAS peaks arising from transitions between surface-modified bands near E_F at the L symmetry point are found to be sensitive to the formation of the surface alloy. The RA response of the c(2×2) surface alloy from 3.0 to 5.5 eV can be simulated using a simple three-phase model based upon the energy derivative of the dielectric function of Cu. The addition of an overlayer phase to this model makes it possible to simulate the higher coverage Si/Cu RA profiles where 1D Si chains cover the surface alloy. The success of the models, in which discrete phases contribute to the RA response, supports the view that the Si chains grow on top of the intact c(2 × 2) alloy, and show that the surface alloy phase and the Si chains persist with further Si deposition. Depositing between 1.2 and 1.8 ML Si results in no change to the RAS signal indicating that the signal remains sensitive to the covered alloy interface.

Acknowledgments

I am grateful to Professor P Weightman (University of Liverpool) for access to UHV experimental facilities. The support of the UK EPSRC is acknowledged.

References

[1] Woodruff D P (ed) 2002 *The Chemical Physics of Solid Surfaces* vol 10 (Amsterdam: Elsevier)
[2] Bardi U 1994 *Rep. Prog. Phys.* **57** 939–87
[3] Rodriguez J A 1996 *Surf. Sci. Rep.* **24** 223
[4] Martín-Gago J A, Fasel R, Hayoz J, Agostino R G, Naumović D, Aebi P and Schlapbach L 1997 *Phys. Rev.* B **55** 12896
[5] Polop C, Rojas C, Román E, Martín-Gago J A, Brena B, Cocco D and Paolucci G 1998 *Surf. Sci.* **407** 268
[6] Rojas C, Polop C, Román E, Martín-Gago J A, Gunnella R, Brena B, Cocco D and Paolucci G 1998 *Phys. Rev.* B **57** 4493
[7] Martín-Gago J A, Rojas C, Polop C, Sacedón J L, Román E, Goldoni A and Paolucci G 1999 *Phys. Rev.* B **59** 3070
[8] Polop C, Sacedón J L and Martín-Gago J A 1998 *Surf. Sci.* **402–404** 245
[9] Rojas C, Palomares F J, López M F, Goldoni A, Paolucci G and Martín-Gago J A 2000 *Surf. Sci.* **454–456** 778
[10] Polop C, Rojas C, Martín-Gago J A, Fasel R, Hayoz J, Naumović D and Aebi P 2001 *Phys. Rev.* B **63** 115414
[11] Magaud L, Sferco S J and Pasturel A 1999 *Phys. Rev.* B **60** 6034
[12] He G, Li S and Zhou Z 2004 *Surf. Sci.* **553** 126
[13] Rojas C, Cerdá J, Jiménez I, Martín M G and Martín-Gago J A 2000 *Surf. Sci.* **466** 144
[14] Aspnes D E, Harbison J P, Studna A A and Florez L T 1988 *J. Vac. Sci. Technol.* A **6** 1327
[15] Martin D S and Weightman P 2004 *Thin Solid Films* **455/456** 752
[16] Weightman P, Martin D S, Cole R J and Farrell T 2005 *Rep. Prog. Phys.* **68** 1251–341
[17] Blanchard N P, Martin D S, Davarpanah A M, Barrett S D and Weightman P 2001 *Phys. Status Solidi* a **188** 1505
[18] Blanchard N P, Martin D S and Weightman P 2004 *Surf. Sci.* **566–568** 837
[19] Martin D S, Blanchard N P and Weightman P 2004 *Phys. Rev.* B **69** 113409
[20] Hofmann Ph, Rose K C, Fernandez V, Bradshaw A M and Richter W 1995 *Phys. Rev. Lett.* **75** 2039
[21] Hansen J-K, Bremer J and Hunderi O 1998 *Surf. Sci.* **418** L58
[22] Sun L D, Hohage M, Zeppenfeld P, Balderas-Navarro R E and Hingerl K 2003 *Surf. Sci.* **527** L184
[23] Martin D S, Cole R J, Blanchard N P, Isted G E, Roseburgh D S and Weightman P 2004 *J. Phys.: Condens. Matter* **16** S4375
[24] Martin D S, Blanchard N P, Weightman P, Roseburgh D S, Cole R J, Hansen J-K, Bremer J and Hunderi O 2007 *Phys. Rev.* B **76** 115403
[25] Winsemius P, van Kampen F F, Lengkeek H P and van Went C G 1976 *J. Phys. F: Met. Phys.* **6** 1583
[26] Monachesi P, Palummo M, Del Sole R, Ahuja R and Eriksson O 2001 *Phys. Rev.* B **64** 115421
[27] Monachesi P, Palummo M, Del Sole R, Grechnev A and Eriksson O 2003 *Phys. Rev.* B **68** 035426
[28] Monachesi P and Chiodo L 2004 *Phys. Rev. Lett.* **93** 116102
[29] Ziane A and Bouarab S 2003 *Phys. Rev.* B **67** 235419
[30] Harl J, Kresse G, Sun L D, Hohage M and Zeppenfeld P 2007 *Phys. Rev.* B **76** 035436
[31] Winsemius P, Lengkeek H P and van Kampen F F 1975 *Physica* B **79** 529
[32] Bremer J, Hansen J-K and Hunderi O 1999 *Surf. Sci.* **436** L735
[33] Martin D S, Cole R J and Weightman P 2005 *Phys. Rev.* B **72** 035408
[34] Dudde R, Bernhoff H and Reihl B 1990 *Phys. Rev.* B **41** 12029
[35] McIntyre J D E and Aspnes D E 1971 *Surf. Sci.* **24** 417
[36] Rossow U, Mantese L and Aspnes D E 1996 *J. Vac. Sci. Technol.* B **14** 3070
[37] Rossow U, Mantese L and Aspnes D E 1998 *Appl. Surf. Sci.* **123/124** 237
[38] Martin D S, Blanchard N P and Weightman P 2003 *Surf. Sci.* **532–535** 1
[39] Isted G E and Martin D S 2005 *Appl. Surf. Sci.* **252** 1883
[40] Stahrenberg K, Herrmann Th, Wilmers K, Esser N, Richter W and Lee M J G 2001 *Phys. Rev.* B **64** 115111
[41] Cole R J, Frederick B G and Weightman P 1998 *J. Vac. Sci. Technol.* A **16** 3088
[42] Heavens O S 1965 *Optical Properties of Thin Solid Films* (New York: Dover)
[43] Fleischer K, Jacob J, Chandola S, Esser N and McGilp J F 2008 *Phys. Status Solidi* c **5** 2556